Journal of Controlled Release 266 (2017) 47–56

Contents lists available at ScienceDirect

Journal of Controlled Release

journal homepage: www.elsevier.com/locate/jconrel

Nanoparticles of a polyaspartamide-based brush copolymer for modified release of sorafenib: *In vitro* and *in vivo* evaluation

Melchiorre Cervello[a,1], Giovanna Pitarresi[b,*,1], Antonella Bavuso Volpe[b], Barbara Porsio[b], Daniele Balasus[a], Maria Rita Emma[a], Antonina Azzolina[a], Roberto Puleio[c], Guido Ruggero Loria[c], Stefano Puleo[d], Gaetano Giammona[a]

[a] *Istituto di Biomedicina e Immunologia Molecolare "Alberto Monroy", Consiglio Nazionale delle Ricerche (CNR), Palermo, Italy*
[b] *Dipartimento di Scienze e Tecnologie Biologiche Chimiche e Farmaceutiche, Università degli Studi di Palermo, Italy*
[c] *Istituto Zooprofilattico Sperimentale della Sicilia "A. Mirri", Area Diagnostica Specialistica, Laboratorio di Istopatologia ed Immunoistochimica, Palermo, Italy*
[d] *Dipartimento di Scienze Mediche, Chirurgiche e Tecnologie Avanzate "G.F. Ingrassia", Università degli Studi di Catania, Italy*

ARTICLE INFO

Keywords:
α-Poly(*N*-2-hydroxyethyl)-D,L-aspartamide
ATRP
Sorafenib
Tumor targeting
Hepatocellular carcinoma

ABSTRACT

In this paper, we describe the preparation of polymeric nanoparticles (NPs) loaded with sorafenib for the treatment of hepatocellular carcinoma (HCC). A synthetic brush copolymer, named PHEA-BIB-ButMA (PBB), was synthesized by Atom Trasnfer Radical Polymerization (ATRP) starting from the α-poly(*N*-2-hydroxyethyl)-D,L-aspartamide (PHEA) and poly butyl methacrylate (ButMA). Empty and sorafenib loaded PBB NPs were, then, produced by using a dialysis method and showed spherical morphology, colloidal size, negative ζ potential and the ability to allow a sustained sorafenib release in physiological environment.

Sorafenib loaded PBB NPs were tested *in vitro* on HCC cells in order to evaluate their cytocompatibility and anticancer efficacy if compared to free drug. Furthermore, the enhanced anticancer effect of sorafenib loaded PBB NPs was demonstrated *in vivo* by using a xenograft model, by first allowing Hep3B cells to grow subcutaneously into nude mice and then administering sorafenib as free drug or incorporated into NPs *via* intraperitoneal injection. Finally, *in vivo* biodistribution studies were performed, showing the ability of the produced drug delivery system to accumulate in a significant manner in the solid tumor by passive targeting, thanks to the enhanced permeability and retention effect.

1. Introduction

Hepatocellular carcinoma (HCC) is one of the most common neoplasm and the third most frequent cause of cancer death, being the leading cause of death among patients with cirrhosis [1].

HCC occurs in people with chronic liver disease, such as chronic viral hepatitis infection (hepatitis B or C), exposure to toxins, aflatoxin or chronic use of alcohol. Certain diseases, such as hemochromatosis and alpha 1-antitrypsin deficiency, markedly increase the risk of developing HCC [1]. HCC is a highly vascularized tumor, the angiogenesis process causes a rapid development of the tumor, followed by invasion and metastasis. Consequently, therapy options for HCC are limited, conventionally divided into curative and palliative. Surgical resection is the major curative technique, but it is very limited for patients with multiple or metastatic tumors. Therefore, it is of great importance to search for effective chemotherapeutic agents to improve the survival rate of patients with advanced or recurrent HCC after surgical treatment [2].

Sorafenib (Fig. 1) is the first drug currently approved by the US Food and Drug Administration (FDA) for the first-line treatment of unrespectable HCC [3]. It is the first therapy to prolong median survival and the time progression by nearly 3 months in HCC patients, representing the new reference standard for the treatment in HCC patients. Although sorafenib is the most promising drug, capable of increasing the overall patient survival, as well as of delaying the progression of the pathology in patients with advanced HCC, its severe systemic side effects (as hand-foot skin reaction, decreased heart blood flow, heart attack, perforation of the bowel, change in thyroid hormone levels, loss of appetite, tiredness, diarrhea, rash, *etc*.) significantly affect patients quality of life and may possibly require the interruption of the treatment. Furthermore, the poor solubility of sorafenib in aqueous environments strongly limits its application.

* Corresponding author at: Dipartimento di Scienze e Tecnologie Biologiche Chimiche e Farmaceutiche, Sezione di Chimica e Tecnologie Farmaceutiche, Università di Palermo, Via Archirafi, 32, 90123 Palermo, Italy.
E-mail address: giovanna.pitarresi@unipa.it (G. Pitarresi).
[1] M. Cervello and G. Pitarresi, contributed equally to this work.

http://dx.doi.org/10.1016/j.jconrel.2017.09.014
Received 21 April 2017; Received in revised form 6 September 2017; Accepted 11 September 2017
Available online 14 September 2017
0168-3659/

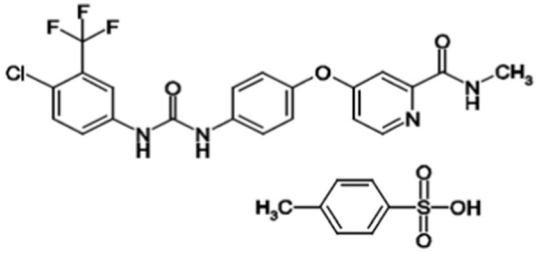

Fig. 1. Chemical structure of sorafenib tosylate.

Some of these problems could be overcome by using polymeric-based nanoparticles (NPs), as evidenced by the strong efforts made by researchers of different fields for the production of drug delivery nanosystems loaded with sorafenib [4–10]. NPs can reach specific sites *via* either active or passive targeting, exploiting in this case the enhanced permeability and retention effect (EPR) [11–15], enhancing the intracellular concentration of drugs in cancer cells, while avoiding toxicity in normal ones. Moreover, NPs show other unique properties as drug delivery systems, like higher therapeutic efficacy, the ability to encapsulate and to release poorly soluble drugs.

In fact, NPs designed to deliver chemotherapeutic agents in cancer therapy, offer many advantages to improve drug delivery and to overcome many problems associated with conventional chemotherapy, improving at the same time the stability, solubility and pharmacokinetics properties of the carried drugs [11].

Being NPs a potential strong platform for a better and more specific delivery of cancer therapeutics, in this work we developed a drug delivery system, based on the synthetic polymer α-poly(*N*-2-hydroxyethyl)-D,L-aspartamide (PHEA) [16,17], loaded with sorafenib for the treatment of HCC. PHEA is a biocompatible water-soluble poly-aminoacidic polymer, whose derivatives have been largely used for tissue engineering [18,19], drug and gene delivery applications [20–25], with a focus for targeted hepatic delivery [6,26].

PHEA was derivatized with α-bromoisobutyryl bromide (BIB), used as a "macroinitiator" for the polymerization *via* Atom Transfer Radical Polymerization (ATRP), and with the hydrophobic monomer butyl methacrylate (ButMA) [27], in order to make the final derivative, PHEA-BIB-pButMA (PBB), suitable for the preparation of NPs. PBB was already used by our research group to encapsulate and release hydrophobic drugs, such as beclomethasone and flutamide, showing its potentiality to produce sorafenib containing particulate systems [28]. Moreover, ATPR technique, a versatile controlled radical polymerization process, enables a precise control of polymer molecular weight, polydispersity index and functionality, making its synthesis easily repeatable.

By using the dialysis method, PBB was employed to produce sorafenib containing NPs, whose properties were studied in terms of particle size and morphology, zeta potential and *in vitro* drug release rate. Cytocompatibility and anticancer efficacy of sorafenib loaded PBB NPs were studied *in vitro* towards human HCC cells (HepG2 and Hep3B). Then, sorafenib loaded PBB NPs were administered parenterally, by using the intraperitoneal route of administration in a xenograft model, obtained by inoculating Hep3B cells in male nude athymic mice. The effect of the produced drug delivery system on the tumor was finally investigated in terms of anticancer efficacy and tumor accumulation.

2. Experimental section

2.1. Materials

The 2-bromoisobutyryl bromide (BIBB), poly butyl methacrylate (pButMA), dimethylamine (DMA), dimethylformamide (DMF), methanol, copper bromide [Cu(I)Br], 2,2[1]-bipyridyl (Bpy) and triethylamine (TEA) were purchased from Sigma-Aldrich (Italy). All reagents were of analytic grade, unless otherwise stated. Monomethyl ether hydroquinone, the stabilizing agent used in the commercial available ButMA, was eliminated through basic activated aluminum oxide column.

Sorafenib tosylate (Fig. 1) was a generous gift of SIFI S.p.A. (Italy).

α,β-poly(*N*-2-hydroxyethyl)-D,L-aspartamide (PHEA) was prepared and purified according to a procedure elsewhere reported [29]. Spectroscopic data (^{1}H NMR) were in agreement with the attributed structure [29]. ^{1}H NMR (300 MHz, D_2O, 25 °C, δ): 2.82 (m, 2H, -CH-*CH_2*-CO-NH-), 3.36 (t, 2H, -NH-*CH_2*-CH_2-OH), 3.66 (t, 2H, -CH_2-*CH_2*-OH), 4.72 (m, 1H, -NH-*CH*-CO-CH_2-).

2.2. Methods

$\overline{M}_w$ of PHEA and PHEA-BIB were determined by Size Exclusion Chromatography (SEC) by using poly (ethylene oxide) standards (range 145–1.5 kDa) were used to obtain the calibration curve. SEC analyses were performed with two ultra-hydrogel columns from Waters (500 and 200 Å) (Milord, MA, USA) connected to a Waters 2410 refractive index detector. A buffer solution at pH 4 was used as an eluent at 37 °C with a flux of 0.8 mL/min. $\overline{M}_w$ of PHEA used in this study, determined by size exclusion chromatography (SEC) analysis, was 42.1 kDa ($\overline{M}_w/\overline{M}_n$ = 1.8).

$\overline{M}_w$and $\overline{M}_w/\overline{M}_n$ of PHEA-BIB-pButMA were determined by SEC in organic media using two Phenogel columns from Phenomenex (10^{4R} and 10^{3R}) connected to a Water 2410 refractive index detector and using a 0.01 M LiBr DMF solution as an eluent with a flow of 0.8 mL/min. The column temperature was set at 50 °C.

^{1}H NMR spectra were obtained by a Bruker Avance II-300 spectrometer, working at 300 MHz.

Mean size (nm) and polydispersity index (PDI) of nanoparticles were determined by photon correlation spectroscopy (PCS) using a Zetasizer Nano ZS (Malvern Instrument, Malvern, U.K.). Measurements were carried out at a fixed angle of 173° at a temperature of 25 °C by using twice-distilled water as dispersing medium.

ζ-potential values (mV) were measured using principles of laser Doppler velocimetry and phase analysis light scattering (M3-PALS technique), calculating these values from the electrophoretic mobility using the Smoluchowsky relationship and assuming that k·a»1 (where k and a are the Debye-Hückel parameter and particle radius, respectively).

2.3. Synthesis of α,β-poly(N-2-hydroxyethyl)-co-[N-2-ethylene(2-bromoisobutyrate)]-D,L-aspartamide (PHEA-BIB) macroinitiator

PHEA-BIB copolymer was synthesized as elsewhere reported [30]. Briefly, PHEA (500 mg; 3.1 mmol of hydroxyethyl-aspartamide repeating units) was dissolved in 10 mL of anhydrous DMA at room temperature, followed by the addition of a suitable amount of TEA (molar ratio between TEA and PHEA equal to 1). BIBB was then added under argon atmosphere (molar ratio between BIBB and PHEA moles equal to 1) maintaining the reaction temperature at 0 °C. Subsequently, the reaction mixture was left at room temperature for 4 h and then precipitated dropwise into diethyl ether. The solid product was washed twice in diethyl ether, dried under vacuum, dialyzed against distilled water (MWCO 12–14 kDa) and freeze-dried.

^{1}H NMR (300 MHz, DMF, 25 °C) δ: 1.90 (s, 6H, CH_3 isobutyril bromide groups), 2.84 (m, 2H, CH2 of PHEA), 3.38 (m, 2H, CH_2 of PHEA), 3.68 (m, 2H, CH_2 of PHEA), 4.33 (m, 2H, CH_2 of PHEA), 4.76 (m, 1H, CH of PHEA).

$\overline{M}_w$ and $\overline{M}_w/\overline{M}_n$ of PHEA-BIB were evaluated by SEC analysis by using the above described method.

2.4. Synthesis of α,β-poly(N-2-hydroxyethyl)-co-{N-2-ethylene-[2-poly (butyl methacrylate)-isobutyrate]}-D,L-aspartamide [PHEA-BIB-pButMA (PBB)] copolymer through ATRP

PHEA-BIB-pButMA (PBB) copolymer was synthesized as elsewhere reported [28,31]. 150 mg of PHEA-BIB (0.255 mmol of side chain BIB groups) were dissolved in a previously degassed 1:1 DMF/MeOH (v/v) mixture (12 mL), then butylmethacrylate was added in order to obtain a molar ratio between butylmethacrylate monomer and BIB in the macroinitiator equal to 10. Later, $Cu^{I}Br$ catalyst (being the molar ratio between $Cu^{I}Br$ and BIB linked group equal to 1) and Bpy (being the molar ratio between the Bpy and BIB linked group equal to 4) were added under continuous stirring and argon bubbling. The reaction solution was left under argon atmosphere at 50 °C for 20 h, and then stopped by opening the reaction vessel until the complete oxidation of copper.

The reaction mixture was precipitated dropwise into a mixture of water:MeOH at the volume ratio 1:1 and the resulting solid residue was washed twice in the same solvent. The white residue was purified by exhaustive dialysis (MWCO 12–14 kDa) and freeze-dried.

^{1}H NMR (300 MHz, DMF, 25 °C, TMS) δ: 1.29 (m, 6H, CH_3 of BIB), 1.56 (m, 2H, CH_2 of ButMA), 1.68 (m, 2H, CH_2 of ButMA), 1.94 (s, 6H, CH_3 of BIB), 2.65 (m, 2H, CH_2 of PHEA), 3.16 (m, 2H, CH_2 of PHEA), 3.41 (m, 2H, CH_2 of PHEA), 3.90 (m, 2H, CH2 of PHEA), 4.13 (m, 2H, CH_2 of PHEA), 4.59 (m, 1H, CH of PHEA).

$\overline{M}_w$ and $\overline{M}_w/\overline{M}_n$ of PBB were evaluated by SEC analysis by using the above described method.

2.5. Preparation of empty and sorafenib loaded PBB nanoparticles

PBB nanoparticles (NPs) were prepared by using a dialysis method. Briefly, PBB copolymer (10 mg) alone or with sorafenib tosylate (6.35 mg) was dissolved in 5 mL of DMF. Copolymer and drug DMF solution was dialyzed (MWCO 100 kDa) at room temperature against 1000 mL of bidistilled water for 24 h, replacing the external aqueous phase at intervals of 3 h. After the dialysis, 10 mg of polyvinylpyrrolidone (PVP) were added as cryoprotectant and the resulting dispersion was finally filtered through 5 μm membrane filter (Sartorius, Minisart Syringe Filter, Germany) and freeze-dried.

2.6. Characterization of PBB NPs

2.6.1. Scanning electron microscopy (SEM)

SEM was performed by using an ESEM Philips XL30 microscope. Sorafenib loaded PBB NPs were dispersed in water and dusted on a double sided adhesive tape previously applied on a stainless steel stub, stored under vacuum for 24 h and sputter-coated with gold prior to microscopy examination.

2.6.2. Dynamic light scattering and ξ-potential analysis

The average size, PDI and ξ-potential of empty and sorafenib loaded NPs were evaluated by using a Malvern Zetasizer Nano ZS instrument. NP dispersions were prepared at the concentration of 0.5 mg/mL in twice-distilled water and analyzed by using the above described method.

2.6.3. Determination of sorafenib content into NPs

The amount of sorafenib into PBB NPs was determined through high-performance liquid chromatography (HPLC) [7], by using an Agilent 1260 Infinity with a multiple wavelength detector, operating at 264 nm, and an Open Lab Chemstation software. The chromatographic procedure was carried out isocratically at 25 °C, using a reverse-phase Gemini C6-phenyl 110A column (Phenomenex 5 μm, 250 × 4.60 mm), methanol–water 90:10 as a mobile phase with a flow rate of 1 mL/min. Sorafenib loaded NPs were suspended in an appropriate amount of methanol and vigorously stirred for 3–4 h for the drug extraction. Resulting solution was centrifuged (6000 rpm for 10 min at 25 °C) and 50 μL of the supernatant was injected into the column.

The obtained peak area, corresponding to sorafenib amount loaded into NPs was compared with a calibration curve obtained by plotting areas *versus* standard solution concentrations of sorafenib in methanol in the range of 0.4–200 μg/mL. The drug loading (DL%) was expressed as the weight percent ratio between the amount of loaded sorafenib and the amount of weighted freeze-dried sorafenib loaded PBB NPs.

2.7. In vitro drug release study

In vitro sorafenib release study was performed by using the dialysis method, under sink conditions, in phosphate buffer solution (PBS) at pH 7.4, in order to simulate physiological fluid.

A known amount of sorafenib loaded PBB NPs was dispersed in 2 mL of PBS, placed into a dialysis tubing (MWCO 12–14 kDa), immersed into 10 mL of PBS containing 1% (v/v) of Tween 80 and then incubated at 37 °C under continuous stirring (100 rpm) in an orbital shaker.

Control experiments were conducted by placing a sorafenib PBS solution into a dialysis tubing (MWCO 12–14 kDa), immersed into 10 mL of PBS containing 1% (v/v) of Tween 80 and then incubated at 37 °C under continuous stirring in an orbital shaker.

Aliquots of the external medium (1 mL) were withdrawn from the outside of the dialysis tubing at fixed time intervals and replaced with equal amounts of fresh medium. Samples were freeze-dried and the amount of sorafenib was detected by HPLC as above reported.

2.8. Cell cultures

The human HCC cell lines HepG2 and Hep3B were obtained from the American Type Culture Collection (ATCC). Cells were cultured at low passage in Roswell Park Memorial Institute (RPMI) medium (SIGMA, Milan, Italy), supplemented with 10% (v/v) Fetal Bovine Serum (FBS) (GIBCO, Life Technologies, Monza MB, Italy), 2 mM L-glutamine, 100 U/mL penicillin-streptomycin and 1 mM sodium pyruvate (all reagents were from SIGMA), in 5% CO_2. All cell lines were routinely screened and confirmed to be negative for mycoplasma contamination.

2.9. Cell viability assays

Cells (5×10^3/well) were plated in 96-well microtiter plates. After 24 h, cells were incubated for 72 h with fresh medium containing: sorafenib tosylate, dissolved in dimethyl sulphoxide (DMSO) at the range concentration of 0.6–10 μM; known amounts of sorafenib loaded PBB NPs corresponding to the entrapped sorafenib concentration in the 0.6–10 μM range and finally empty PBB NPs by using the same concentrations used for sorafenib loaded PBB NPs. Samples were suspended in twice-distilled water in sterile conditions, sonicated for 20 min and diluted with one volume of RPMI complete medium (2 ×). At the end of treatment, MTS assay was performed using the CellTiter Aqueous OneSolution kit (Promega Corporation, Madison, WI, USA) according to the manufacturer's instructions.

Relative cell viability (percentage) was expressed as (Abs_{492} treated cells/Abs_{492} control cells) × 100, on the basis of three experiments conducted in multiple of six. Cells incubated with the medium were used as negative control. In each experiment IC_{50} value was determined as the concentration required to inhibit cell viability by 50%.

2.10. Western blotting analyses

Cells (3×10^5/well) were plated in 6-well microtiter plates and maintained for 24 h. Cells were then treated for 24 h with: sorafenib tosylate, dissolved in DMSO, at the concentration of 2.5, 5 and 7.5 μM; known amounts of sorafenib loaded PBB NPs corresponding to the entrapped sorafenib concentration of 2.5, 5 and 7.5 μM and finally empty

PBB NPs by using the same concentrations used for sorafenib loaded PBB NPs. After treatment, whole cellular lysates were obtained using RIPA buffer (Cell Signaling Technologies Inc., Beverly, MA, USA). Protein concentrations of supernatants were determined with the Bio-Rad protein assay kit (Bio-Rad Laboratories Srl, Milan, Italy) and Western blotting analyses were performed as previously described, with primary antibodies raised against β-actin (SIGMA), ERK1/2, p-ERK1/2, PARP and Mcl-1 (Cell Signaling).

2.11. In vivo studies

Male nude athymic mice (Fox1 nu/nu) 4 weeks old were obtained from Envigo (Udine, Italy) and allowed to acclimatize for 1 week. 0.2 mL of 10 millions Hep3B cells suspensions in PBS, in logarithmic growth phase, were inoculated into the right flank of the animals. When tumors became palpable (around 300 mm^3), mice were randomly divided into four groups of five animals each, with the various tumor volumes equally distributed among four groups. Group one was treated daily (6 days/week) with 10 mg/kg of sorafenib tosylate suspended in DMSO, further diluted in a solution of 25% ethanol (DMSO-EtOH) and administered *via* intraperitoneal injection (IP) injection. Group two received the vehicle alone (DMSO-EtOH). Group three was treated daily (6 days/week) with 10 mg/kg of PBB NPs loaded with sorafenib, suspended in RPMI medium. Group four received empty NPs (PBB alone) suspended in RPMI medium.

Tumor volumes and body weight were recorded twice a week as previously described [32].

Mice were euthanized by cervical dislocation when the tumor burden exceeded 10% of animal body weight, when tumor ulcerated or other conditions of morbidity were ascertained, in conformity with institutional guidelines which are in compliance with national (D.lgs n. 26 4-3-2014) and international laws and policies (ECC Council Directive 86/609, OJ L358.1, 12 December 1987).

At the end of the treatment, tumor, as well as liver, kidneys, lungs and spleen, were collected from each animal. A part of each tumor and organ was frozen in liquid nitrogen and stored at − 80 °C for biodistribution and Western blot analyses, while other parts were fixed in formalin and used for immunohistochemistry analyses.

This study was authorized by the Italian Ministry of Health (No. 1187/2015-PR).

2.12. Immunohistochemistry (IHC) analyses

Immunohistochemical studies on formalin-fixed paraffin-embedded tumor samples were performed as previously described [32]. Mouse monoclonal anti-human CD31 (PECAM-1) (clone 1 A10) was obtained from Leica Biosystems (Newcastle, UK). ImmunoRatio® software was used to quantify Ki-67 expression (http://jvsmicroscope.uta.fi/immunoratio). This software calculates the percentage of positively-stained area (diaminobenzidine (DAB)-stained area) divided by total nuclear area, using a color deconvolution algorithm for separating the staining components (diaminobenzidine and hematoxylin) and adaptive thresholding for nuclear area segmentation.

Percentage of CD31-positive cells was quantified by using ImageJ software (ImageJ – NIH).

2.13. Biodistribution studies

In order to quantify the amount of drug collected into mice organs, sorafenib was extracted by using a procedure elsewhere reported [7]. Each organ sample was mixed with Tris buffer (2 mL, 1 M, pH 8) in a 15 mL glass tube and homogenized by using an Ultraturrax T 25 (Janke & Kunkel Ika - Labortechnik) at 20500 rpm for 15 min. Then, methanol (1 mL) was added to precipitate proteins. Samples were extracted three times with diethyl ether (2 mL), followed by centrifugation at 4000 rpm for 5 min at room temperature. After every solvent addition, the centrifuge tubes were shaken for 15 min at room temperature and centrifuged for 5 min at 4000 rpm. The organic layers were transferred into a glass tube and evaporated to dryness.

Each dried residue was treated with methanol (0.6 mL) and a 50 μL volume was injected into the HPLC system by using conditions above reported.

The extraction efficiency in each organ was previously determined by spiking known amounts of sorafenib in homogenate organs obtained from un-administered animals and by analyzing each mixture as above described.

2.14. Statistical analysis

All the experiments were repeated at least three times. All data are expressed as means ± standard deviation. The statistical analysis was performed by using one way ANOVA with Bonferroni's correction for multiple comparison. A p-value < 0.05 was considered to be indicative of statistical significance, while a p-value < 0.01 was considered as highly significant.

3. Results and discussion

3.1. Synthesis and characterization of PHEA-BIB-pButMA copolymer

The synthetic brush copolymer PHEA-BIB-pButMA (PBB) was synthesized by Atom Trasnfer Radical Polymerization (ATRP). Firstly, PHEA was modified by the conjugation of a proper number of 2-bromoisobutyryl bromide (BIB) residues to the PHEA side chains, obtaining the PHEA-BIB copolymer. In particular, using a molar ratio between the 2-bromoisobutyryl bromide and repeating units of PHEA equal to 1, PHEA-BIB was obtained with a degree of derivatization in BIB equal to 35 mol%. This value was calculated comparing the integral peak, in the ^{1}H NMR of PHEA-BIB, attributable to methyl groups at δ 1.90 of BIB with that assigned of CH_2 of PHEA backbone at δ 3.38 ppm. Weight-average molecular weight ($\overline{M}_w$) of PBB and polydispersity index ($\overline{M}_w/\overline{M}_n$) of PHEA-BIB, evaluated by SEC analysis, resulted to be 48.0 kDa ($\overline{M}_w/\overline{M}_n$ = 1.72).

This first step allowed to obtain a polymeric multifunctional macroinitiator which serves for the subsequent polymerization *via* ATRP of the hydrophobic monomer butyl methacrylate (butMA), making the resulting amphiphilic PBB (Fig. 2) suitable to the production of NPs, thanks to its self-aggregation in aqueous medium [27].

The extension of polymerization process of ButMA has been expressed by means of the average polymerization number, “n”, calculated according to the following equation:

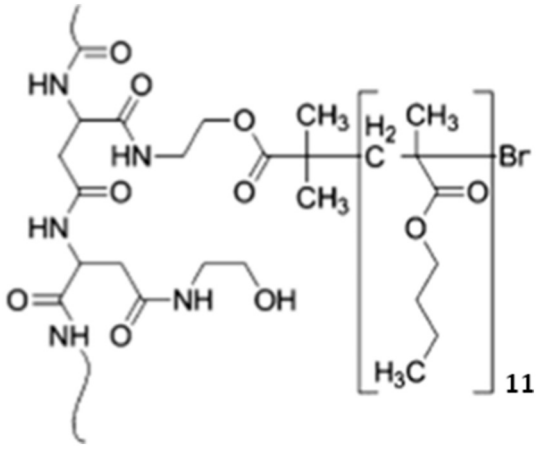

Fig. 2. Chemical structure of PHEA-BIB-pButMA (PBB) copolymer.

$$n \text{ average} = \frac{\text{derivatization degree in ButMA}}{\text{derivatization degree in BIB}}$$

Since the derivatization degree in ButMA was 385 mol% and in BIB was 35 mol%, the "n" average in the final product PHEA-BIB-pButMA resulted to be 11.

Finally, the $\overline{M}_w$ of PHEA-BIB-pButMA (PBB), determined by SEC, was 410 kDa ($\overline{M}_w/\overline{M}_n$ = 2.1). This value is in accordance with the theoretical value calculated for PHEA-BIB-pButMA, considering the starting PHEA and the resulting derivatization degree values in BIB and ButMA, respectively.

3.2. Preparation and characterization of PBB nanoparticles

PBB nanoparticles (NPs) were prepared by using the dialysis method, without the use of any surfactant. PBB copolymer alone or with sorafenib tosylate, dissolved in DMF, was dialyzed for 24 h at room temperature against bidistilled water and with a gentle magnetic stirring to help the diffusion process. After the dialysis, polyvinylpyrrolidone (PVP) was added as a cryoprotectant, and the NP dispersion was finally freeze-dried.

Empty and sorafenib loaded PBB NPs, after re-dispersion in twice-distilled water, were primarily characterized in terms of mean size, polydispersity index and ξ-potential and results are reported in Table 1.

Empty PBB NPs showed a mean diameter of about 196 nm, while the presence of entrapped sorafenib affects this value, being the diameter of sorafenib loaded PBB NPs 240 nm. This size increase is probably ascribable to an enlargement of the particle hydrophobic core due to the presence of the entrapped sorafenib.

ξ-potential values of both empty and drug loaded NPs were negative thus confirming the stability of PBB NPs. Since, ξ-potential does not significantly change after drug incorporation, this result indicates the absence of ionic interactions between sorafenib and PBB NPs.

Morphological characterization was then carried out on PBB/sorafenib NPs by Scanning Electron Microscopy (SEM). SEM image, shown in Fig. 3, highlighted the spherical shape of NPs and confirmed their size, being their diameters similar to the Z-average value obtained from the dynamic light scattering analysis.

The amount of sorafenib entrapped into PBB NPs, expressed as drug loading (DL%) was determined by using an HPLC system and resulted to be 3.8 ± 0.48% w/w.

Moreover, in order to evaluate the physical stability of NPs, aqueous dispersions of sorafenib loaded PBB NPs were dried and then stored at − 20, + 4 and + 25 °C for three months. In all cases, the ratio between the particle size after storage and its initial size was no higher than 1.0 ± 0.1, thus indicating that NPs are stable in all investigated conditions. In addition, it was found that PBB NPs maintained unaltered their amount of entrapped drug at the end of the experiment, being the DL % of freshly prepared sorafenib loaded PBB NPs equal to that obtained at the end of physical stability experiment. These results suggest that physical interactions into PBB NPs are sufficiently strong to confer stability during storage at different temperatures.

3.3. In vitro drug release study

Once incorporated, sorafenib release study from NPs was performed in PBS at pH 7.4 by using the dialysis method, in order to know the ability of produced NPs to retain the incorporate drug in sink conditions and to ensure a sustained release. Because sorafenib is poorly soluble in this medium, 1% (v/v) of Tween 80 was added to the release medium, as a diffusion helping agent.

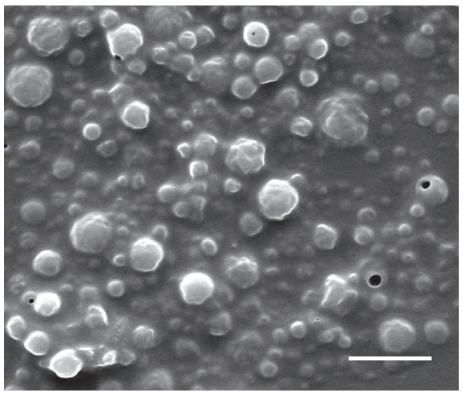

Fig. 3. SEM images of sorafenib loaded PBB NPs (bar represents 500 nm).

The amount of released sorafenib was expressed as percentage ratio between the weight of released drug and the total amount of sorafenib loaded into NPs. Results are reported in Fig. 4.

Results showed that when sorafenib is incorporated in PBB/sorafenib NPs, it is slowly released in the aqueous medium. In fact, after 24 h incubation, the amount of sorafenib released from produced NP sample reached the 55% w/w of the total amount, while at the same incubation time the free drug diffusion through dialysis membrane reached the 100% w/w.

In order to evaluate the *in vitro* drug release data, various kinetics models were used to describe sorafenib release kinetics from produced NPs. Zero-order, First order, Higuchi, Hixson-Crowell, Kormeyer-Peppas and Weibull kinetics models were applied and, on the basis of best fit with the highest correlation value (R^2), it was concluded that sorafenib release from PBB NPs follows the Weibull model (R^2 = 0.9969), described by the equation:

$$F = 100\left[1 - e^{\left(-\frac{(t-T)^b}{a}\right)}\right]$$

where F denotes the amount of drug release at time t, T is the lag time, a denotes a scale parameter, while b describes the shape of the release curve progression [33].

As resulted by kinetics evaluation for sorafenib release from PBB NPs, T resulted to be equal to 0, a and b were 9.22 and 3.10, respectively.

The b coefficient value of the Weibull equation is correlated with the release mechanism of drug from the investigated carrier: if this values is lower than 0.75 the release mechanism is related to Fickian diffusion, while b values between 0.75 and 1.0 suggest that release ranges from Fickian diffusion to case II transport. Being the b coefficient value for PBB/sorafenib NPs higher than 1, it could be concluded that the drug release is driven by a complex mechanism, where erosion of NP matrix and diffusion of drug take place concomitantly.

3.4. In vitro biological studies

In order to evaluate the *in vitro* cytotoxicity effect of free sorafenib,

Table 1
Mean diameter (*Z*-average, nm), polydispersity index (PDI) and ξ-potential in twice-distilled water of empty and sorafenib loaded PBB NPs (PBB/sorafenib).

NPs	Z-average (nm) ± S.D.	PDI ± S.D.	ξ-potential (mV) ± S.D.
PBB	196 ± 7.6	0.32 ± 0.06	− 21.9 ± 4.5
PBB/sorafenib	240 ± 7.7	0.30 ± 0.07	− 28.9 ± 5.7

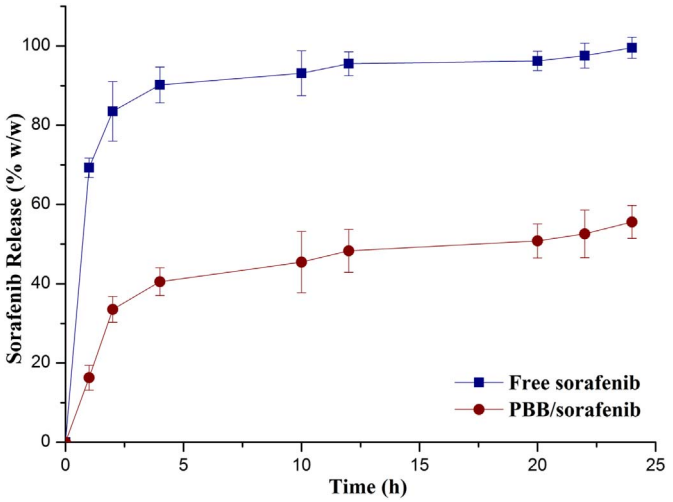

Fig. 4. Profile of free sorafenib dissolution and sorafenib release from PBB/sorafenib NPs in PBS for 24 h.

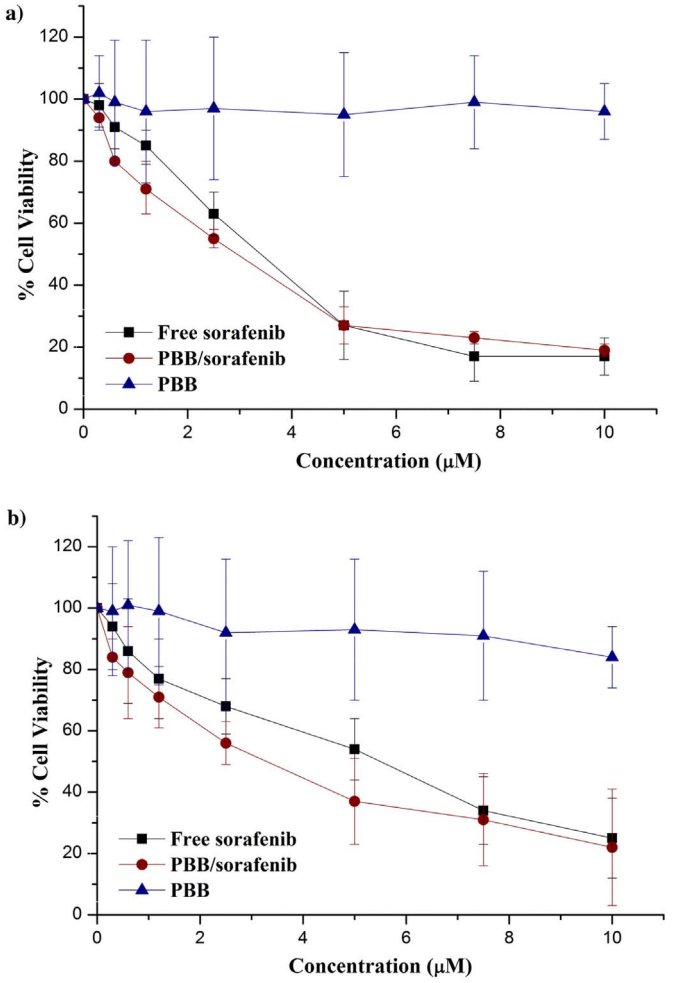

Fig. 5. Effects of free sorafenib, PBB and PBB/sorafenib NPs on cell viability of HepG2 (a) and Hep3B (b) cells.

empty and sorafenib containing PBB NPs, cell viability was evaluated *via* MTS assays towards HepG2 and Hep3 cells (Fig. 5).

After treatment for 72 h with increasing concentration of drug (0.6–10 μM), survival of HCC cells decreases in a dose-dependent manner in the presence of either free sorafenib or PBB/sorafenib NPs. Results demonstrated that sorafenib containing PBB NPs maintain antitumor activity, suggesting that the entrapment of sorafenib into PBB NPs does not cause reduction of drug activity, while slightly reduces cell viability than free drug, as shown by IC_{50} values for both cell lines (Table 2).

Table 2
IC_{50} average values for free sorafenib and PBB/sorafenib NPs.

IC_{50}		
Cells	Free sorafenib (μM) ± S.D.	PBB/sorafenib (μM) ± S.D.
HepG2	5.5 ± 1.0	3.6 ± 1.1
Hep3B	3.5 ± 0.5	3.0 ± 0.3

Therefore, results demonstrate a slight better efficacy of sorafenib containing PBB NPs compared to the free drug, although differences between IC_{50} values are not statistically significant.

On the other hand, very low or no cytotoxic effects of the empty PBB NPs were observed after 72 h in HepG2 and Hep3B cells, respectively (Fig. 5).

3.5. *In vitro evaluation of expression levels of apoptosis-related proteins and signaling molecules*

In order to assess if sorafenib loaded PBB NPs have an antitumor effect comparable to free drug, specific molecular markers were evaluated.

Hep3B cells were grown and treated for 24 h with free sorafenib tosylate, and sorafenib loaded NPs at the drug concentrations of 2.5, 5 and 7.5 μM for 24 h. Empty PBB NPs were used as control, in order to exclude any anticancer activity of the starting polymer. After treatment, cells were harvested and lysed, and equal amounts of extracted proteins were analyzed for expression of poly(ADP)-ribose polymerase (PARP), phospho-ERK1/2 (p-ERK1/2), ERK1/2, myeloid cell leukemia 1 (Mcl-1) proteins by Western blotting.

Data, presented in Fig. 6, are representative of two independent experiments with comparable outcomes.

As shown in Fig. 6, both free sorafenib and sorafenib loaded PBB NPs induced cleavage of PARP at the concentrations of 5 and 7.5 μM. Similarly, the decrease of the p-ERK1/2 signal was evident either after treatment with free sorafenib or with sorafenib loaded NPs PBB, especially at 7.5 μM. PARP is a well-known apoptotic marker, which undergoes proteolytic cleavage after activation of programmed cell death. As it is well known, sorafenib inhibits multiple kinases, including Raf kinase. Inhibition of Raf results in reduction of phosphorylation and

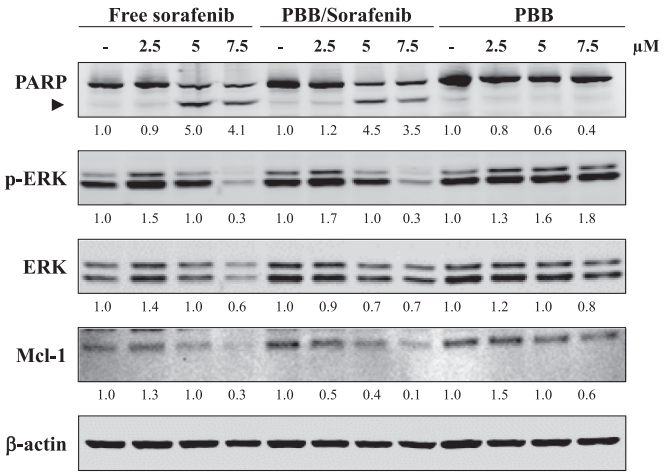

Fig. 6. Effect of free sorafenib, PBB and PBB/sorafenib NPs on apoptosis-related proteins and signaling molecules. The numbers represent the ratio of the relevant protein normalized with β-actin, with vehicle-treated control samples (−) arbitrarily set at 1.0.

activation of the mitogen-activated protein kinases (MAPKs) MEK1/2, which, in turn, cannot phosphorylate and activate the ERK1/2 pathway, essential for cell proliferation, finally leading to a reduction in proliferation rate.

Concerning Mcl-1, inhibition of its expression level is evident at the highest concentrations of both free sorafenib and PBB NPs loaded with drug. Mcl-1 is an anti-apoptotic protein and it has been identified as a downstream target of sorafenib [34,35].

Finally, treatment with empty PBB NPs had no effect in the expression levels of all molecules. These results supported the low *in vitro* cytotoxicity effect of the nanocarrier alone and demonstrated that sorafenib is released from PBB NPs producing its pharmacological effects at the molecular level with the same extent of the free drug.

3.6. In vivo studies

A mouse xenograft tumor model of Hep3B cells was used to assess the *in vivo* efficacy of sorafenib loaded PBB NPs on HCC. When tumors became palpable, at a size of about 300 mm^3, mice were randomized into four groups of five animals each.

Each group was treated for 17 days with free sorafenib, DMSO/EtOH (vehicle, as a control of sorafenib), sorafenib containing PBB NPs and empty PBB (as a control of the loaded NPs), respectively. The sorafenib and PBB/sorafenib treated groups received the drug at 10 mg/kg daily (6 days/week) *via* intraperitoneal injection (IP), while the other two groups received DMSO/EtOH or empty PBB NPs.

At regular time intervals (0, 3, 6, 9, 13 and 17 days) tumor volumes and body weight were recorded, and results, expressed in functions of time, were presented in Fig. 7a and b.

As shown in Fig. 7a, treatment with 10 mg/kg of free sorafenib reduced tumor growth rate compared to DMSO-EtOH, although this difference is not significant.

More interestingly, treatment with sorafenib containing PBB NPs significantly prevented tumor growth compared to the treatment with free drug ($p < 0.05$ at 9 and 13 days, while p is < 0.005 at 17 days).

Concerning changes in animal body weight (Fig. 7 b), mice treated with 10 mg/kg of free sorafenib did not show a significant loss of body weight when compared with mice treated with DMSO/EtOH, suggesting a satisfactory level of drug cytotoxicity at this concentration. On the other hand, mice treated with sorafenib loaded PBB NPs significantly increased their body weight ($p < 0.005$ at 13 days while p is < 0.001 at 17 days), showing also the best physical mobility among the four groups. In summary, sorafenib loaded PBB NPs showed an enhanced *in vivo* efficacy in inhibiting Hep3B cells growth in nude mice compared to the free drug, as well as an improvement of the overall healthiness of the animals.

On the contrary, the decreased body weight observed for the group treated with empty PBB NPs is explained by the absence of any anticancer activity of empty NPs, whose administration to a mouse having a tumor cannot have a positive therapeutic efficacy. As a consequence of this, the decrease in the mice body weight is the normal progression of the cancer disease in the absence of any anticancer treatment.

In Fig. 7c, images of tumors at the end of the 17 days treatment, acquired by using a digital photocamera, were reported and they are representative of all collected tumors.

As evident, PBB/sorafenib NPs caused the most significant tumor dimensions reduction if compared to free sorafenib, empty PBB or DMSO-EtOH.

To evaluate changes in the expression of molecular markers, Western blot analysis was performed on homogenates from tumors obtained from mice after treatments. As shown in Fig. 7d, mice treated with sorafenib containing PBB NPs showed a decrease of p-ERK and Mcl-1 levels than those treated with free drug, empty PBB NPs or DMSO/EtOH. Unexpectedly, we did not observe the cleavage of PARP protein found in *in vitro* studies (data not shown).

These results suggest that *in vivo* other mechanisms may contribute for improved efficacy of sorafenib loaded PBB NPs if compared to free sorafenib. Therefore, the *in vivo* antiproliferative and antiangiogenic activities of free sorafenib and sorafenib containing PBB NPs were determined by immunohistochemical analyses. In particular, to evaluate the antiproliferative activity of the different treatments, expression levels of the nuclear proliferative marker Ki67 were analyzed.

The number of Ki67 positive cells decreases in tumor samples from animals treated with sorafenib containing PBB NPs, compared to that in the tumors of animals treated with free drug, empty PBB NPs or DMSO/EtOH (Fig. 7e).

Moreover, tumor vasculature was evaluated in tumor samples by CD31 staining of blood vessels (Fig. 7f). As shown in Fig. 7f, the number of CD31-positive cells drastically decreases in tumor from animals treated with sorafenib containing PBB NPs, respect to tumors of animals treated with free drug, empty PBB NPs or DMSO/EtOH.

These results suggest that *in vivo* sorafenib entrapped into PBB NPs may act through inhibition of cell proliferation and tumor angiogenesis.

Taken together, these experimental data clearly demonstrated the superior therapeutic efficacy exerted by sorafenib entrapped into PBB NPs respect to free sorafenib.

3.7. Biodistribution studies

In order to evaluate whether the entrapment of sorafenib into PBB NPs could increase the drug targeting to the tumor, *in vivo* biodistribution studies were carried out at the end of the 17 days treatment. During the treatment, mice received 10 mg/kg of drug as free sorafenib or loaded into NPs *via* IP injection. At the end of the administration, the amount of drug in liver, kidneys, lung, spleen and tumor was determined using a HPLC method, as described in the experimental section.

Data, expressed as weight of sorafenib (ng) per each organ weight (mg) and analyzed with ANOVA-Bonferroni test, are reported in Fig. 8.

As shown in Fig. 8, there is an accumulation of sorafenib in various tissues such as liver, spleen, lung and kidneys, but it is evident as it decreased when mice were treated with sorafenib containing PBB NPs. In particular, the amount of sorafenib detected when mice were treated with the free drug is significantly higher in liver ($p < 0.05$), lung and spleen ($p < 0.001$), if compared with sorafenib detected after the injection of drug containing PBB NPs.

On the other hand, sorafenib containing PBB NPs allowed a preferential targeting to the tumor. Indeed, the amount of drug detected in the tumor after the administration of sorafenib containing PBB NPs is markedly higher than that detected after the injection of free sorafenib, and this difference is highly significant ($p < 0.001$).

This preferential accumulation of NPs in the tumor site could be explained by the known enhanced permeation and retention effect (EPR), the most common characteristic that differentiates a tumor from normal healthy tissue [12].

These results show the high potential of sorafenib containing PBB NPs in tumor therapy, since they are able to release the loaded drug preferentially in the tumor site, thus resulting in a marked increase in the drug efficacy and a potential reduction of side effects often due to unspecific and general distribution of the drug to other organs.

4. Conclusions

In this paper, the synthesis of a brush copolymer, named PHEA-BIB-pButMA (PBB) performed by ATRP, is described. The choice of ATRP as a synthetic approach allows to modulate the amount and the length of hydrophobic arms in order to obtained a copolymer able to self-assemble and to form nanoparticles (NPs). In fact, obtained PBB copolymer is able to form core-shell type NPs in an aqueous environment, being PHEA backbone able to form the hydrophilic outer shell, while ButMA arms form the lipophilic core able to entrap hydrophobic drugs.

Sorafenib loaded PBB NPs were prepared by a dialysis method

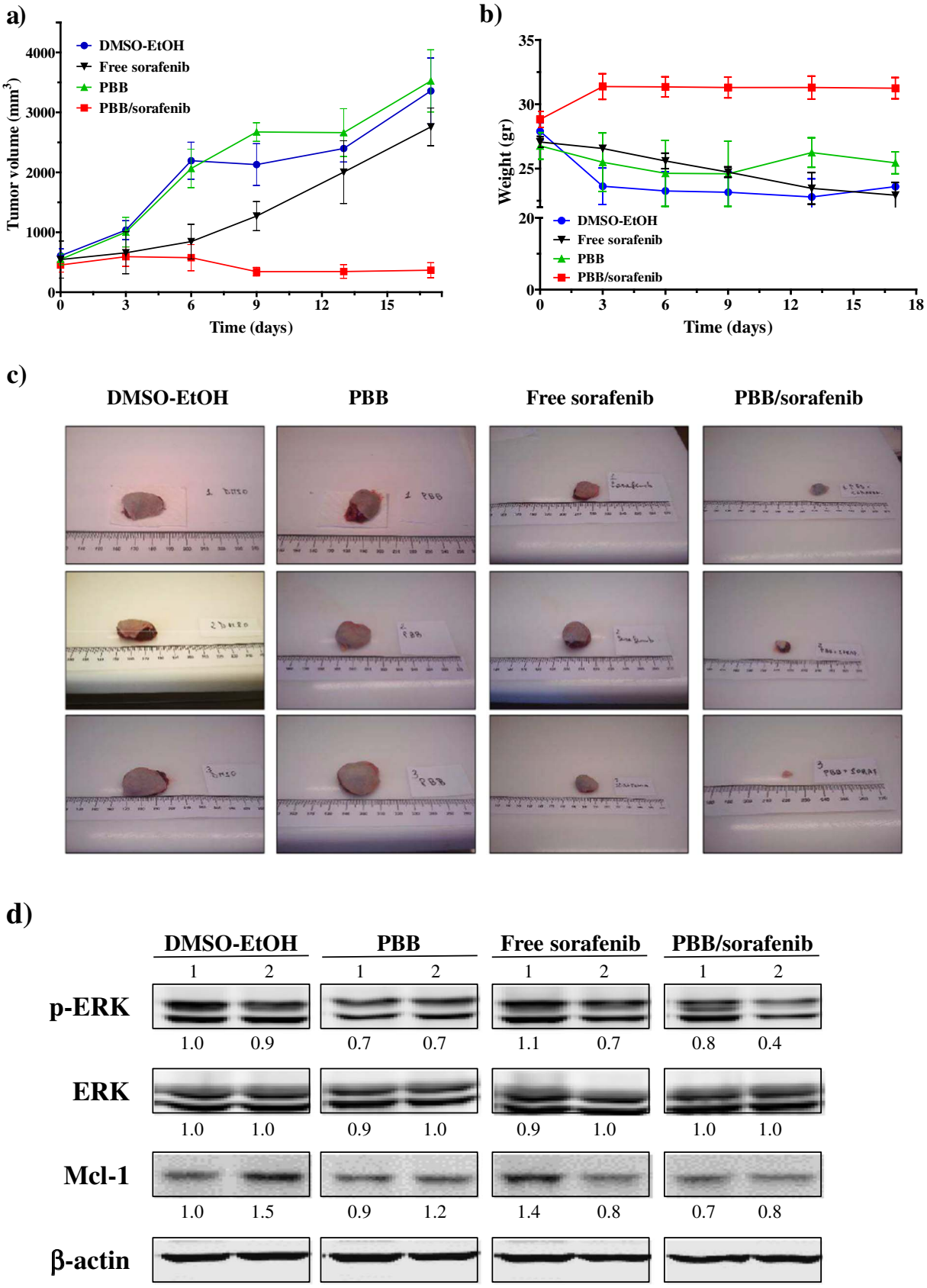

Fig. 7. *In vivo* therapeutic efficacy of sorafenib containing PBB NPs on xenograft models of Hep3B cells. Effect of sorafenib containing PBB NPs on (a) tumor volumes and (b) mice body weights after 3, 6, 9, 13 and 17 days of treatment. (c) Tumor dimension reduction at the end of the 17 days treatment. (d) Representative Western blotting showing phospho-ERK1/2, ERK1/2 and MCl-1 levels in tumor samples. The numbers represent the ratio of the relevant protein normalized with β-actin, with DMOS-EtOH-treated control sample 1 arbitrarily set at 1.0. (e) Immunohistochemical staining of tumor samples for evaluation of Ki-67 proliferation index (scale bar = 50 μm). (f) CD31 staining of blood vessels in tumor samples (scale bar = 50 μm).

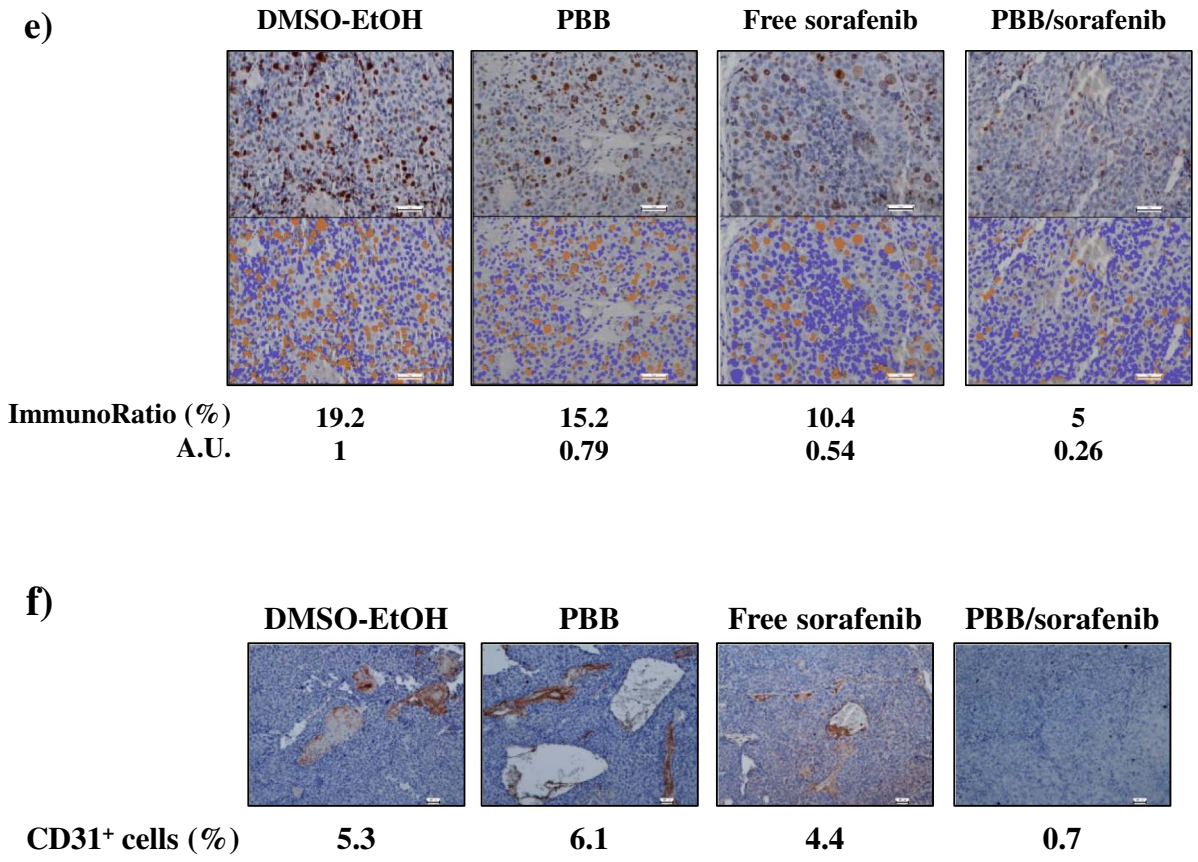

Fig. 7. (*continued*)

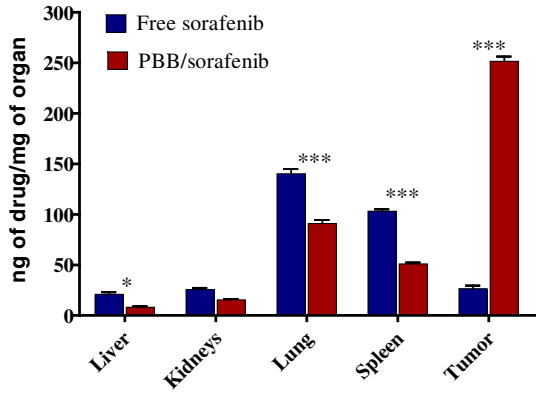

Fig. 8. Sorafenib amount detected in each organs. Results obtained at the end of 17 days treatment, during which mice received 10 mg/kg of free sorafenib or PBB/sorafenib NPs *via* IP injection.

without using any surfactant. Produced NPs were then characterized and showed spherical morphology, 200 nm mean size, negative ξ-potential, and a good ability to entrap the hydrophobic sorafenib. In particular, the inner hydrophobic core of PBB NPs acts as a drug reservoir that causes a retard in drug diffusion in the external medium, as suggested by release study in physiological fluids.

Moreover sorafenib loaded PBB NPs show stable physical properties, such as particle size and drug loading during three months at different storage temperatures.

In vitro biological studies demonstrated a slight better efficacy of sorafenib containing PBB NPs compared to the free drug. Moreover, the use of sorafenib containing PBB NPs in *in vivo* xenograft models showed a significant enhancement of efficacy on the inhibition of tumor growth compared to free drug. Importantly, sorafenib loaded PBB NPs are able to accumulate in a significant manner in the solid tumor mass, whereas their biodistribution in other organs is lower than that showed by sorafenib administered as free drug.

Therefore, PBB NPs represent promising candidates as optimal vehicles for the release of sorafenib in HCC therapy.

Acknowledgements

This work has been funded by MIUR by means of the national Program PON R & C 2007-2013, project Hippocrates – Sviluppo di Micro e Nano-Tecnologie e Sistemi Avanzati per la Salute dell'uomo (PON02_00355_2964193).

References

[1] A. Forner, J.M. Llovet, J. Bruix, J. Bruix, A. Forner, J.M. Llovet, Hepatocellular carcinoma, Lancet 379 (2012) 1245–1255, http://dx.doi.org/10.1016/S0140-6736(11)61347-0.
[2] Z. Xu, L. Chen, W. Gu, Y. Gao, L. Lin, Z. Zhang, Y. Xi, Y. Li, The performance of docetaxel-loaded solid lipid nanoparticles targeted to hepatocellular carcinoma, Biomaterials (2009), http://dx.doi.org/10.1016/j.biomaterials.2008.09.014.
[3] R.C. Kane, A.T. Farrell, R. Madabushi, B. Booth, S. Chattopadhyay, R. Sridhara, R. Justice, R. Pazdur, Sorafenib for the treatment of unresectable hepatocellular carcinoma, Oncologia (2009) 95–100, http://dx.doi.org/10.1634/theoncologist.2008-0185.
[4] A. Grillone, E.R. Riva, A. Mondini, C. Forte, L. Calucci, C. Innocenti, C. de Julian Fernandez, V. Cappello, M. Gemmi, S. Moscato, F. Ronca, R. Sacco, V. Mattoli, G. Ciofani, Active targeting of sorafenib: preparation, characterization, and in vitro testing of drug-loaded magnetic solid lipid nanoparticles, Adv. Healthc. Mater. 4 (2015) 1681–1690, http://dx.doi.org/10.1002/adhm.201500235.
[5] D. Kim, M.-D. Kim, C.-W. Choi, C.-W. Chung, S. Ha, C. Kim, Y.-H. Shim, Y.-I. Jeong, D. Kang, Antitumor activity of sorafenib-incorporated nanoparticles of dextran/poly(dl-lactide-*co*-glycolide) block copolymer, Nanoscale Res. Lett. 7 (2012) 91, http://dx.doi.org/10.1186/1556-276X-7-91.
[6] X. Wang, J. Fan, Y. Liu, B. Zhao, Z. Jia, Q. Zhang, Bioavailability and pharmacokineticss of sorafenib suspension, nanoparticles and nanomatrix for oral administration to rat, Int. J. Pharm. 419 (2011) 339–346, http://dx.doi.org/10.1016/j.ijpharm.2011.08.003.

[7] E.F. Craparo, C. Sardo, R. Serio, M.G. Zizzo, M.L. Bondì, G. Giammona, G. Cavallaro, Galactosylated polymeric carriers for liver targeting of sorafenib, Int. J. Pharm. 466 (2014) 172–180, http://dx.doi.org/10.1016/j.ijpharm.2014.02.047.
[8] H. Zhang, F. Zhang, S. Yan, Preparation, in vitro release, and pharmacokineticss in rabbits of lyophilized injection of sorafenib solid lipid nanoparticles, Int. J. Nanomedicine 7 (2012) 2901, http://dx.doi.org/10.2147/IJN.S32415.
[9] T.T. Lin, D.Y. Gao, Y.C. Liu, Y.C. Sung, D. Wan, J.Y. Liu, T. Chiang, L. Wang, Y. Chen, Development and characterization of sorafenib-loaded PLGA nanoparticles for the systemic treatment of liver fibrosis, J. Control. Release 221 (2016) 62–70, http://dx.doi.org/10.1016/j.jconrel.2015.11.003.
[10] Y. Chen, Y.C. Liu, Y.C. Sung, R.R. Ramjiawan, T.T. Lin, C.C. Chang, K.S. Jeng, C.F. Chang, C.H. Liu, D.Y. Gao, F.F. Hsu, A.M. Duyverman, S. Kitahara, P. Huang, S. Dima, I. Popescu, K.T. Flaherty, A.X. Zhu, N. Bardeesy, R.K. Jain, C.H. Benes, D.G. Duda, Overcoming sorafenib evasion in hepatocellular carcinoma using CXCR4-targeted nanoparticles to co-deliver MEK-inhibitors, Sci Rep 7 (2017) 44123, , http://dx.doi.org/10.1038/srep44123.
[11] A.Z. Wang, R. Langer, O.C. Farokhzad, Nanoparticle delivery of cancer drugs, Annu. Rev. Med. 63 (2012) 185–198, http://dx.doi.org/10.1146/annurev-med-040210-162544.
[12] Y. Matsumura, H. Maeda, A new concept for macromolecular therapeutics in cancer chemotherapy: mechanism of tumoritropic accumulation of proteins and the antitumor agent smancs, Cancer Res. 46 (1986) 6387–6392.
[13] L. Li, W. Sun, L. Li, Y. Liu, et al., A pH-responsive sequential-disassembly nanohybrid for mitochondrial targeting, Nano 9 (2017) 314–325, http://dx.doi.org/10.1039/C6NR07004C.
[14] X. Zhang, K. Achazi, D. Steinhilber, F. Kratz, J. Dernedde, R. Haag, A facile approach for dual-responsive prodrug nanogels based on dendritic polyglycerols with minimal leaching, J. Control. Release 174 (2014) 209–216, http://dx.doi.org/10.1016/j.jconrel.2013.11.005.
[15] Y. Xia, X. Wu, J. Zhao, J. Zhao, Z. Li, W. Ren, Y. Tian, A. Li, Z. Shen, A. Wu, J. Liu, Y.Q. Liu, Y.Z. Hu, X.H. Zhang, M.T. Swihart, P.N. Prasad, Three dimensional plasmonic assemblies of AuNPs with an overall size of sub-200 nm for chemo-photothermal synergistic therapy of breast cancer, Nano 8 (2016) 18682–18692, http://dx.doi.org/10.1039/C6NR07172D.
[16] R. Mendichi, A. Giacometti Schieroni, G. Cavallaro, M. Licciardi, G. Giammona, Molecular characterization of α,β-poly(*N*-2-hydroxyethyl)-dl-aspartamide derivatives as potential self-assembling copolymers forming polymeric micelles, Polymer 44 (2003) 4871–4879, http://dx.doi.org/10.1016/S0032-3861(03)00486-5.
[17] F. Saiano, G. Pitarresi, G. Cavallaro, M. Licciardi, G. Giammona, Evaluation of mucoadhesive properties of α,β-poly(*N*-hydroxyethyl)-dl-aspartamide and α,β-poly (aspartylhydrazide) using ATR–FTIR spectroscopy, Polymer 43 (2002) 6281–6286, http://dx.doi.org/10.1016/S0032-3861(02)00504-9.
[18] G. Pitarresi, C. Fiorica, F.S. Palumbo, S. Rigogliuso, G. Ghersi, G. Giammona, Heparin functionalized polyaspartamide/polyester scaffold for potential blood vessel regeneration, J. Biomed. Mater. Res. Part A. 102 (2014) 1334–1341, http://dx.doi.org/10.1002/jbm.a.34818.
[19] C. Fiorica, F.S. Palumbo, G. Pitarresi, A. Gulino, S. Agnello, G. Giammona, Injectable in situ forming hydrogels based on natural and synthetic polymers for potential application in cartilage repair, RSC Adv. 5 (2015) 19715–19723, http://dx.doi.org/10.1039/C4RA16411C.
[20] G. Pitarresi, P. Pierro, F.S. Palumbo, G. Tripodo, G. Giammona, Photo-cross-linked hydrogels with polysaccharide − poly(amino acid) structure: new biomaterials for pharmaceutical applications, Biomacromolecules 7 (4) (2006) 1302–1310, http://dx.doi.org/10.1021/BM050697M.
[21] G. Giammona, G. Pitarresi, E.F. Craparo, G. Cavallaro, S. Buscemi, New biodegradable hydrogels based on a photo-cross-linkable polyaspartamide and poly (ethylene glycol) derivatives. Release studies of an anticancer drug, Colloid Polym. Sci. 279 (2001) 771–783, http://dx.doi.org/10.1007/s003960100492.
[22] C. Scialabba, F. Rocco, M. Licciardi, G. Pitarresi, M. Ceruti, G. Giammona, Amphiphilic polyaspartamide copolymer-based micelles for rivastigmine delivery to neuronal cells, Drug Deliv. 19 (2012) 307–316, http://dx.doi.org/10.3109/10717544.2012.714813.
[23] N. Mauro, C. Scialabba, G. Cavallaro, M. Licciardi, G. Giammona, Biotin-containing reduced graphene oxide-based nanosystem as a multieffect anticancer agent: combining hyperthermia with targeted chemotherapy, Biomacromolecules 16 (2015) 2766–2775, http://dx.doi.org/10.1021/acs.biomac.5b00705.
[24] E.F. Craparo, B. Porsio, C. Sardo, G. Giammona, G. Cavallaro, Pegylated poly-aspartamide–polylactide based nanoparticles penetrating cystic fibrosis artificial mucus, Biomacromolecules (2016) acs.biomac.5b01480 http://dx.doi.org/10.1021/acs.biomac.5b01480.
[25] E.F. Craparo, B. Porsio, D. Schillaci, M.G. Cusimano, D. Spigolon, G. Giammona, G. Cavallaro, Polyanion–tobramycin nanocomplexes into functional microparticles for the treatment of Pseudomonas aeruginosa infections in cystic fibrosis, Nanomedicine 12 (2017) 25–42, http://dx.doi.org/10.2217/nnm-2016-0262.
[26] E.F. Craparo, G. Teresi, M. Licciardi, M.L. Bondí, G. Cavallaro, Novel composed galactosylated nanodevices containing a ribavirin prodrug as hepatic cell-targeted carriers for HCV treatment, J. Biomed. Nanotechnol. 9 (2013) 1107–1122.
[27] G. Cavallaro, M. Licciardi, M. Di Stefano, G. Pitarresi, G. Giammona, New self-assembling polyaspartamide-based brush copolymers obtained by atom transfer radical polymerization, Macromolecules 42 (2009) 3247–3257, http://dx.doi.org/10.1021/ma8020163.
[28] M. Licciardi, M. Di Stefano, E.F. Craparo, G. Amato, G. Fontana, G. Cavallaro, G. Giammona, PHEA-graft-polybutylmethacrylate copolymer microparticles for delivery of hydrophobic drugs, Int. J. Pharm. 433 (2012) 16–24, http://dx.doi.org/10.1016/j.ijpharm.2012.04.052.
[29] G. Giammona, B. Carlisi, S. Palazzo, Reaction of α,β-poly(*N*-hydroxyethyl)-DL-aspartamide with derivatives of carboxylic acids, J. Polym. Sci. Part A Polym. Chem. 25 (1987) 2813–2818, http://dx.doi.org/10.1002/pola.1987.080251016.
[30] C. Civiale, M. Licciardi, G. Cavallaro, G. Giammona, M.G. Mazzone, Polyhydroxyethylaspartamide-based micelles for ocular drug delivery, Int. J. Pharm. 378 (2009) 177–186, http://dx.doi.org/10.1016/j.ijpharm.2009.05.028.
[31] M. Licciardi, C. Scialabba, C. Fiorica, G. Cavallaro, G. Cassata, G. Giammona, Polymeric nanocarriers for magnetic targeted drug delivery: preparation, characterization, and in vitro and in vivo evaluation, Mol. Pharm. 10 (2013) 4397–4407, http://dx.doi.org/10.1021/mp300718b.
[32] A. Cusimano, R. Puleio, N. D'Alessandro, G.R. Loria, J.A. McCubrey, G. Montalto, M. Cervello, Cytotoxic activity of the novel small molecule AKT inhibitor SC66 in hepatocellular carcinoma cells, Oncotarget 6 (2015) 1707–1722, http://dx.doi.org/10.18632/oncotarget.2738.
[33] S. Dash, P.N. Murthy, L. Nath, P. Chowdhury, Kinetic modeling on drug release from controlled drug delivery systems, Acta Pol. Pharm. 67 (3) (May–Jun 2010) 217–223.
[34] C. Yu, L.M. Bruzek, X.W. Meng, G.J. Gores, C.A. Carter, S.H. Kaufmann, A.A. Adjei, The role of Mcl-1 downregulation in the proapoptotic activity of the multikinase inhibitor BAY 43-9006, Oncogene 24 (2005) 6861–6869, http://dx.doi.org/10.1038/sj.onc.1208841.
[35] L. Liu, Y. Cao, C. Chen, X. Zhang, A. McNabola, D. Wilkie, S. Wilhelm, M. Lynch, C. Carter, Sorafenib blocks the RAF/MEK/ERK pathway, inhibits tumor angiogenesis, and induces tumor cell apoptosis in hepatocellular carcinoma model PLC/PRF/5, Cancer Res. 66 (2006) 11851–11858, http://dx.doi.org/10.1158/0008-5472.CAN-06-1377.